

# Targeted nanoparticle-aptamer bioconjugates for cancer chemotherapy *in vivo*

Omid C. Farokhzad<sup>\*†‡§</sup>, Jianjun Cheng<sup>\*†||</sup>, Benjamin A. Teply<sup>\*†||</sup>, Ines Sherifi<sup>\*†||</sup>, Sangyong Jon<sup>\*\*</sup>, Philip W. Kantoff<sup>††</sup>, Jerome P. Richie<sup>\*\*</sup>, and Robert Langer<sup>†§||</sup>

Departments of <sup>\*</sup>Anesthesiology and <sup>††</sup>Urology, Brigham and Women's Hospital, Harvard Medical School, 75 Francis Street, Boston, MA 02115; <sup>†</sup>Massachusetts Institute of Technology–Harvard Center for Cancer Nanotechnology Excellence, 77 Massachusetts Avenue, Cambridge, MA 02139; <sup>||</sup>Department of Chemical Engineering, Massachusetts Institute of Technology, 77 Massachusetts Avenue, Cambridge, MA 02139; <sup>\*\*</sup>Department of Life Science, Gwangju Institute of Science and Technology, Oryoung-dong, Buk-gu, Gwangju 500-712, Korea; and <sup>††</sup>Lank Center for Genitourinary Oncology, Dana–Farber Cancer Institute, Harvard Medical School, 44 Binney Street, Dana 1230, Boston, MA 02115

Contributed by Robert Langer, March 3, 2006

Targeted uptake of therapeutic nanoparticles in a cell-, tissue-, or disease-specific manner represents a potentially powerful technology. Using prostate cancer as a model, we report docetaxel (Dtxl)-encapsulated nanoparticles formulated with biocompatible and biodegradable poly(D,L-lactic-co-glycolic acid)-*block*-poly(ethylene glycol) (PLGA-*b*-PEG) copolymer and surface functionalized with the A10 2'-fluoropyrimidine RNA aptamers that recognize the extracellular domain of the prostate-specific membrane antigen (PSMA), a well characterized antigen expressed on the surface of prostate cancer cells. These Dtxl-encapsulated nanoparticle-aptamer bioconjugates (Dtxl-NP-Apt) bind to the PSMA protein expressed on the surface of LNCaP prostate epithelial cells and get taken up by these cells resulting in significantly enhanced *in vitro* cellular toxicity as compared with nontargeted nanoparticles that lack the PSMA aptamer (Dtxl-NP) ( $P < 0.0004$ ). The Dtxl-NP-Apt bioconjugates also exhibit remarkable efficacy and reduced toxicity as measured by mean body weight loss (BWL) *in vivo* [body weight loss of  $7.7 \pm 4\%$  vs.  $18 \pm 5\%$  for Dtxl-NP-Apt vs. Dtxl-NP at nadir, respectively (mean  $\pm$  SD);  $n = 7$ ]. After a single intratumoral injection of Dtxl-NP-Apt bioconjugates, complete tumor reduction was observed in five of seven LNCaP xenograft nude mice (initial tumor volume of  $\approx 300$  mm<sup>3</sup>), and 100% of these animals survived our 109-day study. In contrast, two of seven mice in the Dtxl-NP group had complete tumor reduction with 109-day survivability of only 57%. Dtxl alone had a survivability of only 14%. Saline and nanoparticles without drug were similarly nonefficacious. This report demonstrates the potential utility of nanoparticle-aptamer bioconjugates for a therapeutic application.

docetaxel | prostate cancer | targeted delivery | prostate-specific membrane antigen | poly(D,L-lactic-co-glycolic acid) (PLGA)

There has been a substantial interest in developing localized therapeutic options for treatment of early-stage cancer that have reduced toxicity. For example, transperineal ultrasound guided prostate brachytherapy with radioactive <sup>125</sup>I or <sup>103</sup>Pd seeds represents an attractive therapeutic option for low- and intermediate-risk prostate cancer (PCa) patients (1), and its use has increased from 4% in 1993–1995 to 22% in 1999–2001 (2). Despite the rapid adoption of this therapeutic modality, complications still occur, including erectile dysfunction (33–53%) (3), urinary retention (15–32%) (4, 5), and severe radiation-induced bowel injury (1%) (6). Moreover, brachytherapy may fail to eradicate localized prostate cancer, resulting in local recurrence (7).

Nanotechnology approaches where a constant dose of chemotherapy is delivered directly to cancer cells over an extended period may result in alternative or complementary therapeutic options for patients with early-stage cancer. The challenge lies in the design of nanoparticles (NPs) that are specifically and differentially taken up by the targeted cells and release their payload over an extended period to achieve a clinical response (8–10). Using PCa as a model cancer and the following design criteria, we aimed to develop drug-encapsulated NPs for PCa targeting. First, we aimed to

develop NPs using biodegradable and biocompatible components that were previously approved by the Food and Drug Administration (FDA) for a clinical use. We believe that the use of FDA-approved components may facilitate the translation of these vehicles into clinical practice. We chose poly(D,L-lactic-co-glycolic acid) (PLGA) as the controlled release polymer system because its safety in clinical use has been well established, initially as a biomaterial in Vicryl sutures (11) and later as excipients for sustained release of parenteral drugs (12, 13). Second, we aimed to develop NPs that could be surface functionalized with nucleic acid ligands [aptamers (Apts)] for targeted delivery and uptake in a cell-specific manner. Aptamers are DNA or RNA oligonucleotides that, through intramolecular interactions, fold into unique tertiary conformations capable of binding to target antigens with high affinity and specificity, analogous to antibodies (14, 15). We chose Apts as targeting molecules because this class of ligands is nonimmunogenic and exhibits remarkable stability in a wide range of pH ( $\approx 4$ –9), temperature, and organic solvents without loss of activity (16, 17). Furthermore, Apt synthesis does not rely on biological systems and is an entirely chemical process that can decrease batch-to-batch variability when production is scaled up. These characteristics are in contrast to antibodies that may be immunogenic or more labile, and their large-scale biological production is prone to significant batch-to-batch variability (18, 19). Third, we aimed to develop NPs that resist uptake by tissue macrophages and by nontargeted cells, thus increasing their residence time at the site of administration. We chose to develop poly(ethylene glycol) (PEG)-functionalized NPs because we had previously shown that pegylated polymeric NPs are considerably more effective against systemic clearance than similar particles without PEG (20, 21). PEG has also been used to improve the pharmacokinetic properties of liposomes (22), macromolecules (23), and small molecule drugs (24). Fourth, we aimed to develop NPs that demonstrate differential cytotoxicity against PCa *in vitro* and *in vivo* using a chemotherapeutic agent currently in clinical use for the management of PCa. Docetaxel (Dtxl), when used systemically, can prolong the survival of patients with hormone-resistant PCa (25, 26). We postulated that controlled release of Dtxl targeted to PCa cells may result in enhanced cytotoxicity and antitumor efficacy, making it a potential therapeutic modality for the management of localized prostate cancer. The combination of the above

Conflict of interest statement: No conflicts declared.

Abbreviations: PCa, prostate cancer; Dtxl, docetaxel; NP, nanoparticle; Apt, aptamer; PLGA, poly(D,L-lactic-co-glycolic acid); PEG, poly(ethylene glycol); PSMA, prostate-specific membrane antigen; H&E, hematoxylin/eosin; BWL, body weight loss.

<sup>†</sup>O.C.F., J.C., and B.A.T. contributed equally to this work.

<sup>§</sup>To whom correspondence may be addressed. E-mail: ofarokhzad@partners.org or rlander@mit.edu.

<sup>||</sup>Present address: Department of Materials Science and Engineering, University of Illinois at Urbana–Champaign, 1304 West Green Street, Urbana, IL 61801.

© 2006 by The National Academy of Sciences of the USA

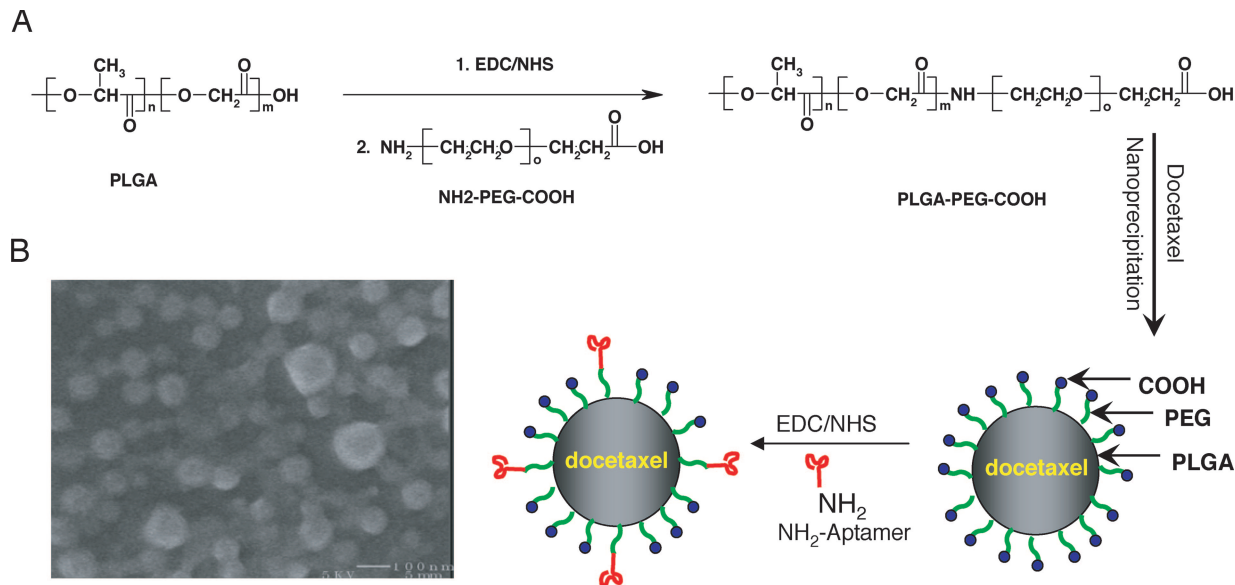


**Fig. 1.** Development of Dtxl-encapsulated pegylated PLGA NP-Apt bioconjugates. (A) Schematic representation of the synthesis of PLGA-PEG-COOH copolymer and strategy of encapsulation of Dtxl. We developed Dtxl-encapsulated, pegylated NPs by the nanoprecipitation method. These particles have a negative surface charge attributable to the carboxylic acid on the terminal end of the PEG. The NPs were conjugated to amine-functionalized A10 PSMA Apt by carbodiimide coupling chemistry. (B) Representative scanning electron microscopy image of resulting Dtxl-encapsulated NPs is shown. EDC, 1-ethyl-3-(3-dimethylaminopropyl)-carbodiimide; NHS, *N*-hydroxysuccinimide.

design criteria may facilitate the translation of therapeutically effective NP-Apt bioconjugates into clinical practice.

We had previously encapsulated rhodamine-labeled dextran (as a model drug) within NPs formulated with poly(D,L-lactic acid) (PLA)-*b*-PEG block copolymer and surface functionalized these NPs with nuclease-stabilized A10 2'-fluoropyrimidine RNA Apts (27) that recognize the extracellular domain of the prostate-specific membrane antigen (PSMA) (28–31). PSMA is a well characterized antigen expressed on the surface of PCa cells that participates in membrane recycling and becomes internalized through ligand-induced endocytosis (32, 33). Our data demonstrated that these fluorescently labeled, targeted NP-Apt bioconjugates differentially bound and got taken up by LNCaP prostate epithelial cells, which express the PSMA protein efficiently and with high specificity. No binding or uptake was detected in PC3 prostate epithelial cells, which do not express the PSMA protein (34, 35).

Herein, we developed Dtxl-encapsulated, pegylated PLGA NP-Apt bioconjugates that bind to the PSMA protein on the surface of PCa cells. We assessed the efficacy of these bioconjugates *in vitro* and *in vivo* using a LNCaP xenograft nude mouse model of PCa. We now report an example of NP-Apt bioconjugates that exhibit significant anticancer efficacy without the systemic toxicity that is common to chemotherapeutics.

## Results and Discussion

**Development of NPs.** We used the nanoprecipitation method (36) to encapsulate Dtxl within PLGA-*b*-PEG block copolymer with a terminal carboxylic acid group (PLGA-PEG-COOH) and developed Dtxl-encapsulated, pegylated PLGA NPs [ $153.3 \pm 13.9$  nm (mean  $\pm$  SD);  $n = 10$ ] (Fig. 1A). The hydrophilic PEG group facilitates the presentation of the carboxylic acid on the NP surface. Additionally, the PEG group decreases nonspecific biofouling of particles *in vivo* (37) and minimizes the particle uptake by nontargeted cells, including their premature clearance by the mononuclear phagocytic system (21, 38). The presence of the carboxy-modified PEG on the NP surface also results in a negative surface charge [ $\zeta$  potential,  $-42 \pm 1$  mV (mean  $\pm$  SD);  $n = 3$ ] that may decrease nonspecific interaction of the negatively charged Apts with the NP surface, thus preserving Apt conformation and binding character-

istics (34). The surface of these NPs was functionalized with the A10 PSMA Apt (27) to allow differential uptake by targeted PCa cells. The surface morphology and size distribution of NPs were evaluated by scanning electron microscopy (SEM) (Fig. 1B). The functionalization of the NPs with Apt resulted in an  $\approx 15$ -nm increase in particle size, presumably attributed to the presence of Apts on the NP surface.

**In Vitro Cellular Cytotoxicity Assays (MTT Assays).** We examined the *in vitro* differential cytotoxicity of Dtxl-encapsulated, pegylated PLGA NP-Apt bioconjugates (Dtxl-NP-Apt) vs. similar NPs lacking the A10 PSMA Apt (Dtxl-NP) using LNCaP cells, which express the PSMA protein. Because Dtxl is a hydrophobic and membrane-permeable drug and because PSMA has been shown

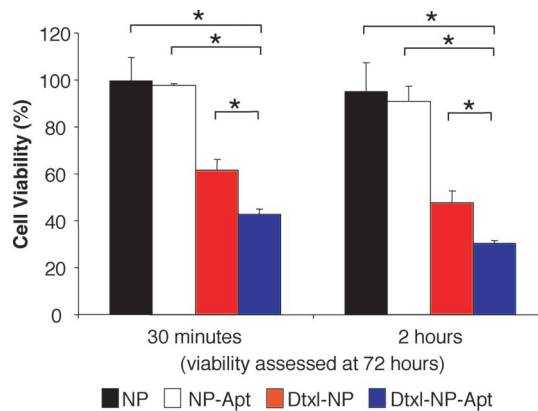


**Fig. 2.** MTT assay to determine the differential cytotoxicity of Dtxl-encapsulated NP-Apt bioconjugates (Dtxl-NP-Apt), Dtxl-encapsulated NPs lacking the A10 PSMA Apt (Dtxl-NP), control NP-Apt bioconjugates without Dtxl (NP-Apt), and control NPs without Dtxl (NP) after incubation with LNCaP prostate epithelial cells. NPs were incubated with cells for 30 min (Left) or 2 h (Right), and the cells were subsequently washed and incubated in media for a total of 72 h before assessing cell viability in each group. \*, Significance by ANOVA at 95% confidence interval.



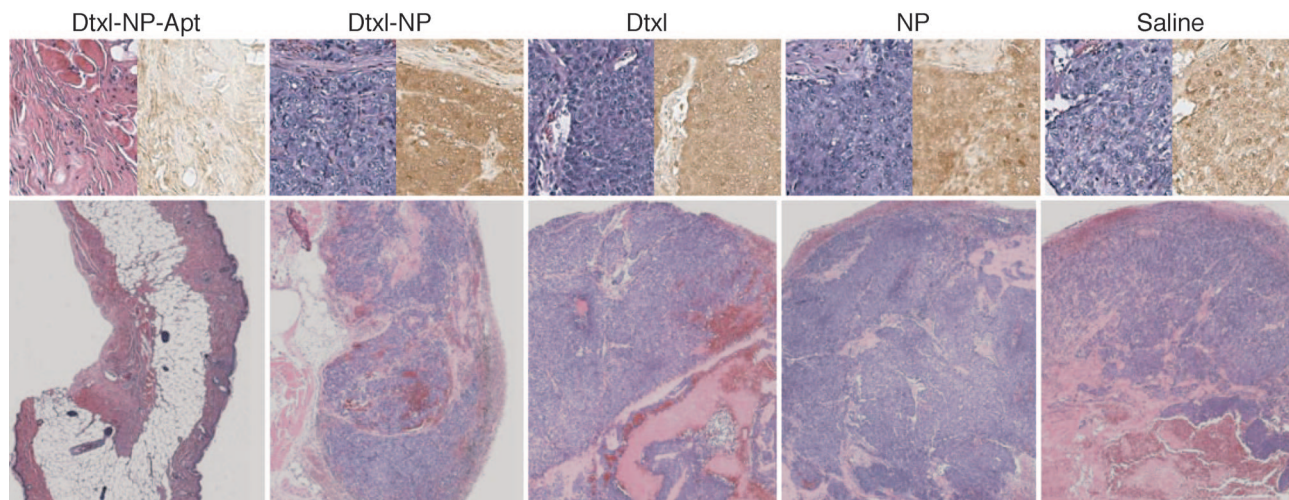


**Fig. 4.** Histological staining of the excised tumors in the (i) saline, (ii) pegylated PLGA NP without drug (NP), (iii) emulsified Dtxl (Dtxl), (iv) Dtxl-encapsulated NPs (Dtxl-NP), or (v) Dtxl-encapsulated NP-Apt bioconjugates (Dtxl-NP-Apt) was evaluated by an independent pathologist. The larger images (Lower) are H&E staining of representative specimens at  $\times 20$  magnification. The smaller images (Upper) are H&E (Left) and PSMA (Right) staining of consecutive sections for each group at  $\times 50$  magnification. All specimens except those obtained from the Dtxl-NP-Apt-treated mice were positive for PSMA staining [dark brown horseradish peroxidase stain]. The Dtxl-NP-Apt staining confirmed the absence of residual tumor and presence of scar and adipose tissue.

not show any long-term efficacy, and the mean tumor sizes at the end of the study for the groups were  $786 \pm 7 \text{ mm}^3$ ,  $775 \pm 25 \text{ mm}^3$ , and  $741 \pm 40 \text{ mm}^3$ , respectively (mean  $\pm$  SEM;  $n = 7$ ). None of the animals of the saline and NP groups exhibited tumor regression. Overall five of seven animals in the saline group and six of seven animals in the NP group reached end point (defined as excessive tumor load of  $>800 \text{ mm}^3$  or body weight loss (BWL) of  $>20\%$ ) during the 109-day study duration. The remaining three animals in these two groups failed to reach the end point during the study, an observation that is consistent with the well documented slow rate of LNCaP tumor growth, which is also characteristic of PCa growth in humans. Six of the seven animals in the Dtxl cohort reached the end point. The difference in the final mean tumor size or survival time for the Dtxl group compared with the saline and NP groups was not statistically significant (ANOVA at 95% confidence interval).

The Dtxl-NP-Apt-treated group demonstrated the most dramatic efficacy: the final mean tumor load was  $119 \pm 84 \text{ mm}^3$  (mean  $\pm$  SEM;  $n = 7$ , significantly smaller than all other groups by ANOVA at 95% confidence interval). In total, five of seven treated animals experienced complete tumor reductions on days 25, 25, 31, 37, and 40. The remaining two animals also exhibited regression of their tumor size after the initial dosing, and one of these two animals experienced progression after the initial regression and had a tumor size of  $567 \text{ mm}^3$  by the end of the study (Fig. 3C). All mice in the Dtxl-NP-Apt group survived the 109-day study duration. The Dtxl-NP group was also more efficacious than the Dtxl, NP, and saline control groups, but significantly less efficacious when compared with the Dtxl-NP-Apt group. The mean tumor size at end point was  $315 \pm 103 \text{ mm}^3$  (mean  $\pm$  SEM;  $n = 7$ ). Two complete tumor reductions were observed on days 31 and 43, and the tumor size in one animal reached end point on day 73. The study demonstrated that, after a single administration, the Dtxl-NP-Apt group was most efficacious against LNCaP PCa tumors, resulting in a better survival than other treatment groups (Fig. 3D).

We next performed histological staining of the excised tumors and the tissue at the injection sites, and the slides were evaluated by an independent pathologist (Fig. 4). The complete reduction of tumor and presence of fibrotic tissue in the median tumors of the Dtxl-NP-Apt group was confirmed by hematoxylin/eosin (H&E) staining and negative PSMA staining, consistent with the elimination of LNCaP tumor mass. In the remaining groups, the H&E and

PSMA staining of the median tumors at end point demonstrated positive PSMA staining, with areas of hemorrhagic necrosis consistent with the presence of tumors (Fig. 4).

We assessed toxicity of each group *in vivo* by analyzing their effect on the WBC count and BWL. The assessment of the WBC count in all five groups at the end point confirmed no evidence of leukopenia or associated toxicities (Fig. 5A). The NP and saline groups demonstrated a BWL trend that roughly paralleled their tumor load. These control groups did not experience any acute depression in body weight after dosing, which is consistent with the absence of drug in the formulations. One animal in each of the saline and Dtxl groups experienced  $>20\%$  BWL, respectively, on day 44 ( $755 \text{ mm}^3$ ) and day 95 ( $539 \text{ mm}^3$ ), possibly due to tumor load of these animals. The Dtxl-NP group had two animals with excessive BWL ( $>20\%$ ), which were euthanized on days 9 and 12. The average weights of the other animals in the Dtxl-NP cohort returned to predosing levels by day 26. At nadir, the Dtxl-NP group exhibited a maximal mean BWL of  $18 \pm 5\%$  (mean  $\pm$  SD;  $n = 7$ ) on day 12 (Fig. 5B). The Dtxl mean BWL at nadir was  $17 \pm 3\%$  (mean  $\pm$  SD;  $n = 7$ ) on day 8 and by day 19, the mean body weight had recovered to predosing levels. A statistically significant smaller maximal mean BWL of  $7.7 \pm 4.0\%$  (mean  $\pm$  SD;  $n = 7$ ) was observed for the Dtxl-NP-Apt group on day 6, with recovery to its original mean body weight on day 19 (Fig. 5B). The observed acute BWL and subsequent recovery after dosing of the Dtxl-NP-Apt and Dtxl-NP groups may represent bulk degradation of PLGA, resulting in a burst followed by slower continued release of Dtxl over time. This release pattern is characteristic of the PLGA controlled release polymer system and allows for the presence of the Dtxl over an extended period at the site of administration. Our *in vitro* drug release assays demonstrate that  $\approx 20\%$  of the drug is yet to be released after 1 month of incubation in an aqueous solution (data not shown).

One possible explanation for significantly enhanced efficacy and a relatively smaller BWL in the Dtxl-NP-Apt group as compared with the Dtxl-NP group may be that the former group is expected to get internalized into tumor cells with subsequent intracellular release of the drug. The latter may release the drug in the extracellular space, causing systemic absorption and distribution, increased toxicity, and decreased efficacy. The nontargeted NPs may also diffuse away from the tumor site and release the drug after concentrating in other organs, possibly underlying the early mor-

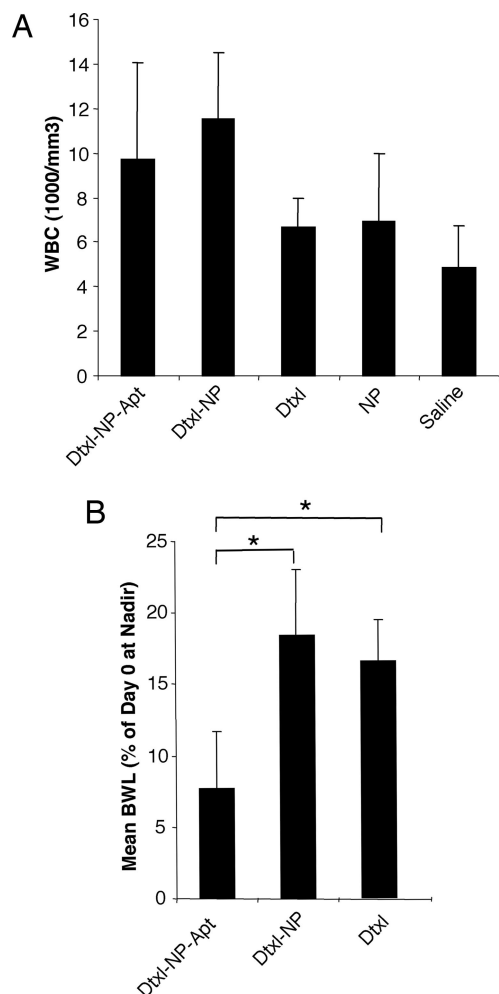


**Fig. 5.** Evaluation of treatment toxicity. (A) WBC counts at the experimental end point were within the normal range for all groups and confirmed the absence of persistent hematologic toxicity. (B) Mean BWL after dosing of mouse in each group is shown. \*, Significant difference by ANOVA at 95% confidence interval.

bidity in two animals of the cohort. This explanation would be consistent with our own and other investigators' *in vitro* findings that PSMA is constitutively endocytosed and that the targeting of this molecule results in the intracellular delivery of the PSMA ligands (33, 34, 41). For example, the J591 antibody, which recognizes the extracellular domain of the PSMA, has been shown to specifically bind to LNCaP cells and get rapidly internalized and accumulate in the endosomes through a clathrin-mediated pathway (33). Additionally, we have shown that the A10 PSMA Apt-functionalized NPs are taken up by LNCaP cells whereas similar NPs lacking the PSMA Apt remain extracellular (34). These data, however, were generated by using *in vitro* models, and any *in vivo* correlation would need further evaluation.

It is also possible that the differential toxicity of the Dtxl-NP-Apt bioconjugates is due to their interaction with the tumor microenvironment in such a way as to lead to enhanced efficacy and/or decreased toxicity through a mechanism that is independent of their binding to the PSMA protein on the PCa cells. For example, it has been shown that both particle size and charge play a role in passive tumor targeting of systemically administered NPs and that cationic (42) and smaller (43) particles are better at concentrating in the tumors vs. similarly designed anionic and larger particles. Although we are not aware of previous studies suggesting that these param-

eters are also important in clearance of particles from tumor after intratumoral delivery, it is nonetheless possible that the presence of Apts on the surface of NPs may have altered the surface charge or size of the Dtxl-NP-Apt bioconjugates in a way to lead to a lower rate of lymphatic or systemic clearance of these particles from the tumor interstitium, leading to enhanced efficacy as compared with the Dtxl-NP group.

A thorough evaluation of these alternative possibilities to explain the dramatic efficacy of Dtxl-NP-Apt bioconjugate vs. other groups will require similar *in vivo* efficacy studies using LNCaP xenograft models that are deficient in PSMA expression or development and testing of similar Dtxl-NP-Apt bioconjugates using random Apts that lack specificity for the PSMA protein.

**Summary.** We had previously developed proof of concept drug delivery vehicles that were composed of polymeric NPs and Apts for targeted delivery and uptake by PCa cells (34). Herein, we have demonstrated *in vitro* and *in vivo* efficacy of NP-Apt bioconjugates against cancer cells. These bioconjugates have the advantage that the materials used in the development of the NPs were approved by the Food and Drug Administration for a prior clinical use and that the targeting molecules used in their development are small, relatively stable, nonimmunogenic, and easy to synthesize, which together may facilitate the translation of these bioconjugates into clinical practice. We postulate that a similar approach may be used to develop therapeutic and diagnostic NP-Apt bioconjugates for other important human diseases.

#### Materials and Methods

**Materials.** All chemicals were obtained from Sigma-Aldrich unless otherwise noted. PLGA [inherent viscosity 0.20 dl/g in hexafluoroisopropanol (HFIP)] with acid end groups was purchased from Absorbable Polymers International (Pelham, AL). The heterofunctional PEG polymer with a terminal amine and carboxylic acid functional groups (NH<sub>2</sub>-PEG-COOH) was custom synthesized (molecular weight = 3,400; Nektar Therapeutics, San Carlos, CA).

**Synthesis of PLGA-PEG-COOH Block Copolymer.** The PLGA-COOH and NH<sub>2</sub>-PEG<sub>3400</sub>-COOH polymers were used to synthesize PLGA-*b*-PEG copolymer with terminal carboxylic acid groups (PLGA-PEG-COOH). PLGA-COOH was preactivated to its succinimide by using 1-ethyl-3-(3-dimethylaminopropyl)-carbodiimide (EDC) and *N*-hydroxysulfosuccinimide (sulfo-NHS) and then reacted with NH<sub>2</sub>-PEG-COOH. The resulting PLGA-PEG-COOH was characterized by <sup>1</sup>H-NMR (400 MHz, CDCl<sub>3</sub>), δ 5.19 (m br, -C(O)CH(CH<sub>3</sub>)O-), 4.79 (m br, -C(O)CH<sub>2</sub>O-), 3.62 (m, -OCH<sub>2</sub>CH<sub>2</sub>-), 3.43 (m, -OCH<sub>2</sub>CH<sub>2</sub>-), 1.54 (m, -C(O)CH(CH<sub>3</sub>)O-).

**Development of Dtxl-Encapsulated NPs.** Dtxl-encapsulated NPs were prepared by using the nanoprecipitation method. Briefly, PLGA-PEG-COOH (10 mg/ml) and Dtxl (0.5 mg/ml) were dissolved in acetonitrile and together mixed dropwise into water, giving a final polymer concentration of 3.3 mg/ml. The NPs were stirred for 1 h, and the remaining organic solvent was removed in a rotary evaporator at reduced pressure. The NPs were centrifuged at 10,000 × *g* for 15 min and washed with deionized water, and the size (in nanometers) and surface charge (ζ-potential in millivolts) of NPs were evaluated by Quasi-elastic laser light scattering (QELS) by using a ZetaPALS dynamic light-scattering detector (15 mW laser, incident beam = 676 nm; Brookhaven Instruments, Holtsville, NY). Surface morphology and size were also determined by high-resolution scanning electron microscopy (JEOL 6320FV). Dtxl content in the NPs for calculation of dosing quantity was determined on an Agilent (Palo Alto, CA) 1100 HPLC equipped with a pentafluorophenyl column (Curosil-PFP, 250 × 4.6 mm, 5 μ; Phenomenex, Torrance, CA) by using a UV detector at 227 nm.

**NP-Apt Conjugation.** The PLGA-PEG-COOH NP suspension ( $\approx 10 \mu\text{g}/\mu\text{l}$  in DNase RNase-free water) was incubated with 400 mM 1-ethyl-3-(3-dimethylaminopropyl)-carbodiimide and 100 mM *N*-hydroxysuccinimide for 15 min at room temperature with gentle stirring. The resulting *N*-hydroxysuccinimide-activated particles were covalently linked to 5'-NH<sub>2</sub> modified A10 PSMA Apts (2% weight compared with polymer concentration). The resulting NP-Apt were washed, resuspended in PBS, and used immediately.

**In Vitro Cytotoxicity Assays.** The prostate LNCaP cells were grown in 12-well plates in RPMI medium 1640 (American Type Culture Collection), supplemented with 100 units/ml aqueous penicillin G, 100  $\mu\text{g}/\text{ml}$  streptomycin, and 10% FBS at concentrations to allow 70% confluence in 24 h (i.e., 40,000 LNCaP cells per  $\text{cm}^2$ ). On the day of experiments, cells were washed with prewarmed PBS and incubated with prewarmed phenol-red reduced OptiMEM media for 30 min before the addition of 0.6  $\mu\text{g}/\text{ml}$  Dtxl-NP or Dtxl-NP-Apt. The control cells were incubated with NP and NP-Apt without Dtxl. Cells were incubated for 30 min or 2 h at 37°C and washed three times with PBS (100  $\mu\text{l}$ ), and fresh growth media were replaced in the plates. The cells were incubated for a total of 72 h. Cell viability was assessed colorimetrically with MTT reagent (Invitrogen). One-way ANOVA with Fisher's least significant difference (LSD) post hoc comparisons at 95% confidence interval was used for statistical comparisons.

**In Vivo Efficacy Studies.** Animals were cared for under the supervision of the Massachusetts Institute of Technology Division of Comparative Medicine and in compliance with the Principles of Laboratory Animal Care of the National Institutes of Health. PSMA-expressing xenograph flank tumors were induced in 8-week-old BALB/c nude mice by s.c. injection of 3 million LNCaP cells suspended in 1:1 media and matrigel. After 3 weeks when tumors had reached  $\approx 300 \text{ mm}^3$ , mice were divided into five groups of seven mice, minimizing weight and tumor size differences. Tumor-bearing nude mice were treated by intratumoral injection of emulsified Dtxl

(40 mg/kg), Dtxl-NP-Apt (40 mg/kg), Dtxl-NP (40 mg/kg), NP without drug (NP), or saline. After dosing, the mice were monitored for weight and implanted tumor size daily for 2 weeks and every 3 days thereafter. If BWL persisted beyond 20% of predosing weight, the animals were euthanized. The length and width of the tumors were measured by digital calipers, calculating tumor volume by the following formula:  $(\text{width}^2 \times \text{length})/2$ . Mice were monitored for a maximum of 109 days, until the tumor was completely regressed or until the tumor volume exceeded 800  $\text{mm}^3$ , for which the mice were euthanized for excessive tumor load. For animals that were euthanized because of tumor load or BWL, the tumor size at the time of euthanasia was used for the purpose of mean tumor size calculation. Initial volume of the tumors averaged 328  $\text{mm}^3$ . Average body weight for mice in the study was 19.2 g. One-way ANOVA with Fisher's LSD post hoc comparisons at 95% confidence interval was used for statistical comparisons.

**Histology.** After antigen retrieval, formalin-fixed and paraffin-embedded (FFPE) tissue slides from median tumors in each group were incubated with biotin-labeled A10 PSMA Apt in 1 ml of PBS in the presence of  $5 \times$  molar excess of tRNA and 0.2% BSA for 30 min at 37°C. Slides were washed three times with PBS and incubated with horseradish peroxidase (HRP)-conjugated streptavidin for 5 min, washed three times with PBS, incubated with the peroxidase substrate, washed twice with PBS, mounted, and analyzed by light microscopy. H&E staining was performed by the Massachusetts Institute of Technology Division of Comparative Medicine.

We thank Drs. Chris Cannizzaro, Etgar Levy-Nissenbaum, Y. Z. Wang, Kris Wood, Ali Khademhosseini, Robert Ross, and Meredith Regan for helpful discussions and Dr. Arlin Rogers for evaluation of histological slides. This work was supported by National Institutes of Health (NIH)/National Cancer Institute Grant CA 119349, by NIH/National Institute of Biomedical Imaging and Bioengineering Grant EB003647, and by the David Koch Cancer Research Fund.

- Grimm, P. D., Blasko, J. C., Sylvester, J. E., Meier, R. M. & Cavanagh, W. (2001) *Int. J. Radiat. Oncol. Biol. Phys.* **51**, 31–40.
- Cooperberg, M. R., Moul, J. W. & Carroll, P. R. (2005) *J. Clin. Oncol.* **23**, 8146–8151.
- Teloken, C. (2001) *Cancer Control* **8**, 540–545.
- Han, B. H., Demel, K. C., Wallner, K., Ellis, W., Young, L. & Russell, K. (2001) *J. Urol.* **166**, 953–957.
- Bucci, J., Morris, W. J., Keyes, M., Spadinger, I., Sidhu, S. & Moravan, V. (2002) *Int. J. Radiat. Oncol. Biol. Phys.* **53**, 91–98.
- Shah, S. A., Cima, R. R., Benoit, E., Breen, E. L. & Bleday, R. (2004) *Dis. Colon Rectum* **47**, 1487–1492.
- Peschel, R. E. & Colberg, J. W. (2003) *Lancet Oncol.* **4**, 233–241.
- Ferrari, M. (2005) *Nat. Rev. Cancer* **5**, 161–171.
- Langer, R. (1998) *Nature* **392**, 5–10.
- Langer, R. (2001) *Science* **293**, 58–59.
- Saunders, R. A. & Helveston, E. M. (1979) *Ophthalmic Surg.* **10**, 13–18.
- Caron, P. (2002) *Ann. Endocrinol. (Paris)* **63**, 2S19–2S24.
- Guerin, C., Olivi, A., Weingart, J. D., Lawson, H. C. & Brem, H. (2004) *Invest. New Drugs* **22**, 27–37.
- Ellington, A. D. & Szostak, J. W. (1990) *Nature* **346**, 818–822.
- Tuerk, C. & Gold, L. (1990) *Science* **249**, 505–510.
- Nimjee, S. M., Rusconi, C. P. & Sullenger, B. A. (2005) *Annu. Rev. Med.* **56**, 555–583.
- Wilson, C. & Szostak, J. W. (1998) *Chem. Biol.* **5**, 609–617.
- Cheifetz, A. & Mayer, L. (2005) *Mt. Sinai J. Med.* **72**, 250–256.
- Chester, K., Pedley, B., Tolner, B., Violet, J., Mayer, A., Sharma, S., Boxer, G., Green, A., Nagl, S. & Begent, R. (2004) *Tumour Biol.* **25**, 91–98.
- Gref, R., Minamitake, Y., Peracchia, M. T., Domb, A., Trubetskoy, V., Torchilin, V. & Langer, R. (1997) *Pharm. Biotechnol.* **10**, 167–198.
- Gref, R., Minamitake, Y., Peracchia, M. T., Trubetskoy, V., Torchilin, V. & Langer, R. (1994) *Science* **263**, 1600–1603.
- Moghimi, S. M. & Szebeni, J. (2003) *Prog. Lipid Res.* **42**, 463–478.
- Christie, R. J. & Grainger, D. W. (2003) *Adv. Drug Deliv. Rev.* **55**, 421–437.
- Pechar, M., Ulbrich, K., Subr, V., Seymour, L. W. & Schacht, E. H. (2000) *Bioconjug. Chem.* **11**, 131–139.
- Petrylak, D. P., Tangen, C. M., Hussain, M. H., Lara, P. N., Jr., Jones, J. A., Taplin, M. E., Burch, P. A., Berry, D., Moynour, C., Kohli, M., et al. (2004) *N. Engl. J. Med.* **351**, 1513–1520.
- Tannock, I. F., de Wit, R., Berry, W. R., Horti, J., Pluzanska, A., Chi, K. N., Oudard, S., Theodore, C., James, N. D., Turesson, I., et al. (2004) *N. Engl. J. Med.* **351**, 1502–1512.
- Lupold, S. E., Hicke, B. J., Lin, Y. & Coffey, D. S. (2002) *Cancer Res.* **62**, 4029–4033.
- Leach, F. (2004) *Cancer Biol. Ther.* **3**, 559–560.
- Murphy, G. P., Elgamal, A. A., Su, S. L., Bostwick, D. G. & Holmes, E. H. (1998) *Cancer* **83**, 2259–2269.
- Thomas, T. P., Patri, A. K., Myc, A., Myaing, M. T., Ye, J. Y., Norris, T. B. & Baker, J. R., Jr. (2004) *Biomacromolecules* **5**, 2269–2274.
- Slovin, S. F. (2005) *Expert Opin. Ther. Targets* **9**, 561–570.
- Ghosh, A. & Heston, W. D. (2004) *J. Cell. Biochem.* **91**, 528–539.
- Liu, H., Rajasekaran, A. K., Moy, P., Xia, Y., Kim, S., Navarro, V., Rahmati, R. & Bander, N. H. (1998) *Cancer Res.* **58**, 4055–4060.
- Farokhzad, O. C., Jon, S., Khademhosseini, A., Tran, T. N., Lavan, D. A. & Langer, R. (2004) *Cancer Res.* **64**, 7668–7672.
- Farokhzad, O. C., Khademhosseini, A., Jon, S., Hermmann, A., Cheng, J., Chin, C., Kiseluyuk, A., Teply, B., Eng, G. & Langer, R. (2005) *Anal. Chem.* **77**, 5453–5459.
- Chorny, M., Fishbein, I., Danenberg, H. D. & Golomb, G. (2002) *J. Controlled Release* **83**, 389–400.
- Burchenal, J. E., Deible, C. R., Deglau, T. E., Russell, A. J., Beckman, E. J. & Wagner, W. R. (2002) *J. Thromb. Thrombolysis* **13**, 27–33.
- Owens, D. E., III, & Peppas, N. A. (2006) *Int. J. Pharm.* **307**, 93–102.
- Horoszewicz, J. S., Leong, S. S., Kawinski, E., Karr, J. P., Rosenthal, H., Chu, T. M., Mirand, E. A. & Murphy, G. P. (1983) *Cancer Res.* **43**, 1809–1818.
- Vanhoefer, U., Cao, S., Harstrick, A., Seeber, S. & Rustum, Y. M. (1997) *Ann. Oncol.* **8**, 1221–1228.
- Rajasekaran, S. A., Anilkumar, G., Oshima, E., Bowie, J. U., Liu, H., Heston, W., Bander, N. H. & Rajasekaran, A. K. (2003) *Mol. Biol. Cell* **14**, 4835–4845.
- Campbell, R. B., Fukumura, D., Brown, E. B., Mazzola, L. M., Izumi, Y., Jain, R. K., Torchilin, V. P. & Munn, L. L. (2002) *Cancer Res.* **62**, 6831–6836.
- Kong, G., Braun, R. D. & Dewhirst, M. W. (2000) *Cancer Res.* **60**, 4440–4445.